CHALMERS
UNIVERSITY OF TECHNOLOGY

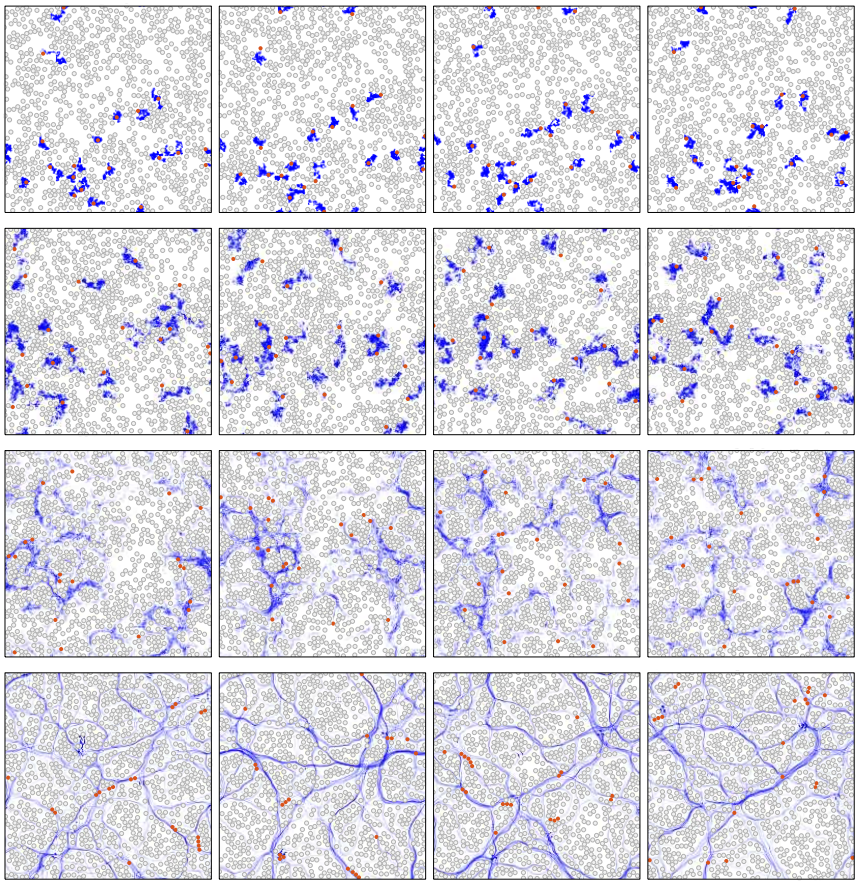

Collective Dynamics in a Complex Environment

Master's thesis in Complex Adaptive Systems

Simon Nilsson

Department of Physics
Chalmers University of Technology
Gothenburg, Sweden 2017

Master's thesis 2017

Collective Dynamics in a Complex Environment

SIMON NILSSON

CHALMERS
UNIVERSITY OF TECHNOLOGY

Department of Physics
Soft Matter Lab
Chalmers University of Technology
Gothenburg, Sweden 2017

Collective Dynamics in a Complex Environment
SIMON NILSSON

Supervisor: Giovanni Volpe, Department of Physics, University of Gothenburg
Examiner: Giovanni Volpe, Department of Physics, University of Gothenburg

Master's Thesis 2017
Department of Physics
Soft Matter Lab
Chalmers University of Technology
SE-412 96 Gothenburg
Telephone +46 31 772 1000

Cover: The emergence of metastable channels in a system of active and passive particles (increasing time going left to right) as noise decreases in the system (top to bottom). Figure constructed from results from simulations done in Matlab.

Typeset in LaTeX
Gothenburg, Sweden 2017

Abstract

Collective behaviour is a phenomenon that often occurs in systems of many interacting individuals. Common macroscopic examples of collective behaviour are flocks of birds, swarms of insects and crowds of people. On the microscopic scale, it is often observed in so-called active systems, constituted by self-propelled particles, also known as active particles. Motile bacteria or synthetic microswimmers are among the most commonly studied active particles.

The potential applications of collective behaviour and understanding thereof encompass multiple disciplines, ranging from robotics and medicine to algorithms, like ant colony optimization. However, the apparent complexity makes understanding an intimidating task. Despite this, simple models have proven successful in capturing the defining characteristics of such systems.

This thesis examines a well-known model of active matter and expands it to incorporate necessary components to explore the effects a complex environment has on this pre-existing model. Additionally, a new model is proposed and explored in purely active systems as well as in complex environments. Simulations show that a phase transition between a gaseous state and the formation of metastable clusters occurs as the level of orientational noise decreases. Furthermore, they show that this model describes the formation of metastable channels in a crowded environment of passive particles.

Sammanfattning

Fenomenet kollektivt beteende uppkommer ofta i system av många, interagerande individer. Vanliga makroskopiska exempel på kollektivt beteende är fågelflockar, insektssvärmar och folkmassor. På den mikroskopiska skalan observeras ofta kollektivt beteende i aktiva system, bestående av självdrivna partiklar, s.k. aktiva partiklar. Till de mest studerade aktiva partiklarna hör rörliga bakterier och syntetiska mikrosimmare ("microswimmers" i litteraturen).

Potentiella applikationer baserade på kollektivt beteende sträcker sig över ett flertal discipliner, däribland robotik och medicin samt algoritmer, som myrkolonioptimering. Komplexiteten dessa system uppvisar gör dock att det kan kännas som en skrämmande uppgift att försöka förstå och beskriva dem. Trots detta har mycket enkla modeller visat sig fånga flera av de karakteristiska drag kollektivt beteende har.

Det här arbetet undersöker en välkänd modell av aktiv materia och bygger vidare på den, för att fånga nödvändiga aspekter då modellen studeras i en mer komplex miljö. Dessutom presenteras en ny modell som utforskas, med hjälp av simuleringar, i helt aktiva system liksom i komplexa miljöer. Simuleringarna visar att en fasövergång sker, mellan ett gaslikt tillstånd och bildandet av metastabila kluster, då mängden orienteringsbrus minskar. Ytterligare visar de att modellen beskriver bildandet av metastabila kanaler i en miljö fylld av passiva partiklar.

Contents

List of Figures

Chapter 1

Introducing Collective Dynamics and Active Particles

This first chapter introduces the subject of collective behaviour, its applications and some key principles when modelling collective behaviour and complex systems. It also introduces active particles, or self-propelled particles, as a means to study and apply collective behaviour on the microscopic scale. If you, the reader, have prior knowledge on the subject, feel free to skip ahead to Chapter 2.

1.1 Introduction to Collective Dynamics and Complex Systems

Collective behaviour occurs on many length and time scales, with many examples from everyday life, such as herds of animals, flocks of bird, swarms of insects or bacteria and human crowds (Vicsek and Zafeiris, 2012; Gautrais et al., 2012). Typically, collective behaviour emerges in systems of interacting individuals capable of motion. The resulting behaviour displays a high degree of complexity, despite the constituent individuals often being very simple by themselves.

Collective behaviour in nature can have specific tasks. These tasks are often carried out with very high efficiency, such as that of ants gathering food, despite the lack of inherent leaders or individuals being aware of an overall plan (Wahde, 2008). For this reason, collective behaviour has inspired a wide range of optimization algorithms, e.g. ant colony optimization (Wahde, 2008). Apart from in algorithms, knowledge of collective behaviour has contributed in fields like medicine, swarm robotics, autonomous vehicles and computer graphics (Wang and Gao, 2012; Brambilla et al., 2013; Reynolds, 1987).

The first model of collective behaviour was created by Reynolds (1987) to simulate something looking like a flock of birds in computer graphics. It proved very successful, despite its simplicity. Later, Vicsek et al. (1995) built upon this to create a very well-known model in the field. The same model will be used later in this thesis.

The complexity of collective behaviour poses a daunting task for our understanding, but as shown by Reynolds (1987) and Vicsek et al. (1995), the defining characteristics can often be captured by very simple models. This has become one of the main principles for modelling complex systems. In fact, simple models have several advantages. Firstly, simpler models often mean that they are less computationally intensive, which in turn means that numerical simulations can be done faster and larger systems can be simulated within feasible time frames. It is also cost efficient and better suited for real-world implementations. Secondly, simpler models often describe phenomena more concisely, due to necessity. This naturally leads to the third major point; simple models are easier to understand and therefore more can be gained from studying them, as they encompass the "purest" description of underlying mechanisms.

1.2 Active Matter: Collective Dynamics on the Microscale

On the microscopic scale collective behaviour is observed in active systems, consisting of active particles, also commonly known as self-propelled particles (Bechinger et al., 2016). Active particles are capable of converting energy from their environment to propel themselves, hence the name.

As a result of the self-propulsion, active particles operate far from thermal equilibrium, giving rise to many interesting phenomena not displayed by passive systems. For example, active particles are able to form clusters without having attracting forces between them, as shown in simulations by Peruani et al. (2006). The most commonly studied active particles are motile bacteria and fabricated microswimmers and many such systems exhibiting collective behaviour have been realised experimentally. Motile bacteria have been known to form vortices and other spatial patterns (Czirók et al., 1996) and artificial active particles have been shown to cluster and form crystal-like structure (Theurkauff et al., 2012; Palacci et al., 2013; Ginot et al., 2015).

In the future, possible applications in medicine for collective behaviour and active particles could be personalised medical care with highly accurate cancer treatments, where the active agents target and kill cancer cells selectively, or drug delivery systems via active particles, for increased precision and efficiency. Before this can become a reality, however, suitable biocompatible active systems must be developed for use in the human body, as pointed out by Bechinger et al. (2016). Furthermore, we need a better understanding of their behaviour in complex and crowded environments and how to exploit it (Bechinger et al., 2016). The aim of this thesis is to study collective behaviour in complex environments, which is done via numerical simulations.

Chapter 2

The Vicsek Model

This second chapter will introduce the Vicsek model, a well-known model of self-organization in active particles. After explaining it in detail, a modification incorporating important aspects for examining it in a complex environment will also be presented and compared to the original model. This modification gives each particle a finite size and is then used in later parts of the work to study the collective behaviour in complex environments.

2.1 Original Model

The original model was presented in the paper "Novel Type of Phase Transition in a System of Self-Driven Particles" by Vicsek et al. in 1995 and concerns self-propelled particles, or active particles. In a very simple way, Vicsek's model manages to capture important characteristics of collective behaviour using aligning interactions between self-propelling particles similar to the famous Boids model by Reynolds (1987). In these models, each particle's behaviour is based on its perception of the local environment (Reynolds, 1987; Bechinger et al., 2016).

The Vicsek model considers a set of N active particles moving continuously in a two-dimensional, square space with periodic boundaries. In the particle interaction dynamics proposed by Vicsek et al., each particle is propelled with a constant speed v and tends to align its direction with the local neighbours. The local neighbours are defined as all particles (including the particle itself) that are found within a circle of radius r centred on the particle in question. Other works have explored other options, such as using a "vision cone" (Barberis and Peruani, 2016), where the full circle of the Vicsek model is a special case.

For a set of N particles with positions $\mathbf{x}_i$ and velocities $\mathbf{v}_i = v(\cos\theta_i, \sin\theta_i)^T$, $i = 1, \ldots, N$, the orientation and position of each particle are updated from one timestep to the next according to

$$\begin{aligned} \theta_i(t+1) &= \langle\theta(t)\rangle_r + \xi \\ \mathbf{x}_i(t+1) &= \mathbf{x}_i(t) + \mathbf{v}_i\left(\theta_i(t+1)\right), \end{aligned} \tag{2.1}$$

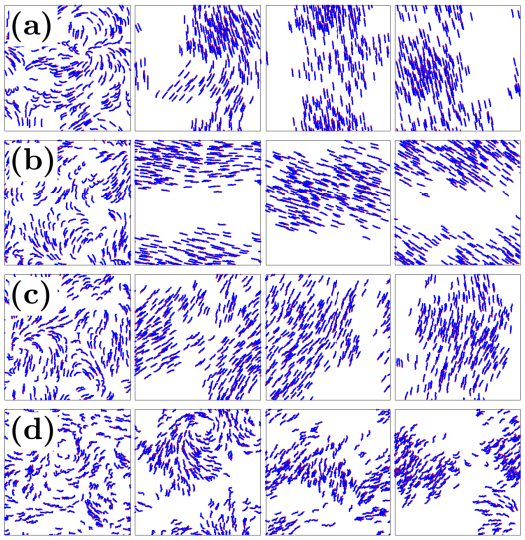

Figure 2.1: 400 particles have been simulated on a square with the side $L = 10$ and periodic boundary conditions using the Vicsek model. The panels, left to right, correspond to times 20, 100, 500 and 1 000. Noise levels in the simulations shown above are (a) $\eta = 0.03\pi$, (b) $\eta = 0.15\pi$, (c) $\eta = 0.3\pi$ and (d) $\eta = 0.6\pi$ respectively. Increasing the noise, a transition from macroscopic order to varied but correlated movement occurs. Particles are marked by red dots and particle trails are shown in blue.

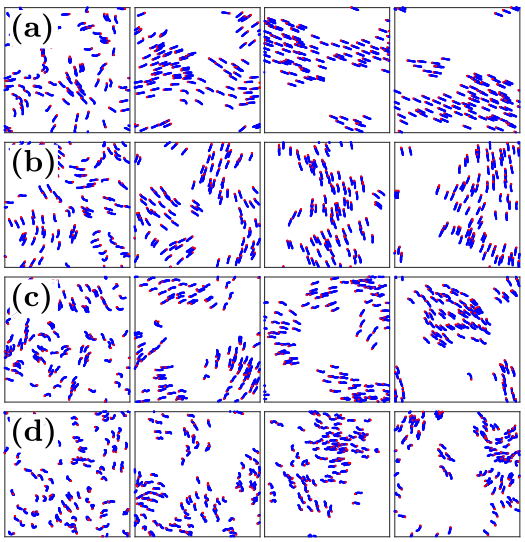

Figure 2.2: 100 particles have been simulated on a square with the side $L = 10$ and periodic boundary conditions using the Vicsek model. The panels, left to right, correspond to times 20, 100, 500 and 1 000. Noise levels in the simulations shown above are (a) $\eta = 0.03\pi$, (b) $\eta = 0.15\pi$, (c) $\eta = 0.3\pi$ and (d) $\eta = 0.6\pi$ respectively, as in Figure 2.1. For lower densities, as noise increases, macroscopic order or large clusters transitions to smaller clusters, where clusters merge and break off more frequently than at higher densities. Again, particles are marked in red and particle trails are shown in blue.

where ξ is a white noise term uniformly distributed on the interval $[-\eta/2, \eta/2]$ and

$$\langle\theta\rangle_r = \arctan\left(\frac{\langle\sin\theta\rangle_r}{\langle\cos\theta\rangle_r}\right). \tag{2.2}$$

Here, $\langle\cdot\rangle_r$ denotes the average taken over all particles within a radius of r.

Vicsek et al. (1995) found that, depending on the level of noise η and the particle density, different behaviours were observed. Mainly, four regions were identified. With low noise levels and high concentration of particles the system reaches a macroscopic, system-wide order where all particles move in a spontaneously chosen direction. For higher levels of noise the order is broken and varied but correlated motion emerges, where particles move in large clusters. Figure 2.1 shows computer simulations for different noise levels at high particle concentration.

At lower concentrations, particles tend to move in clusters in random directions that occasionally merge with other colliding clusters. Since groups of particles are very unlikely to break off from the cluster, this system also reaches an "ordered" state, but after much longer times. Increasing the noise levels at lower densities increases the likelihood of particles breaking off from clusters and consequently the clusters are smaller and shorter-lived. Additionally, clusters more frequently change direction. Figure 2.2 shows simulation results for such systems.

The system reaches some ordered state at sufficiently low levels of noise, regardless of density-regime. This is characterized by a system-wide direction of motion. This contrasts with a maximally unordered system where all particles' directions of motion are completely uncorrelated. To quantify how ordered a system is, the observable order parameter v_a, the averaged normalized velocity (Vicsek et al., 1995), is defined as

$$v_\mathrm{a} = \frac{1}{Nv}\left|\sum_{i=1}^{N}\mathbf{v}_i\right|. \tag{2.3}$$

By design, a maximally ordered system will have an order parameter of unity and the completely disordered system will have $v_\mathrm{a} = 0$. All other systems will have a $v_\mathrm{a} \in (0, 1)$.

Comparing the average normalized velocity v_a for different noise levels η, a clear phase transition from ordered to unordered is observed. This is shown in Figure 2.3.

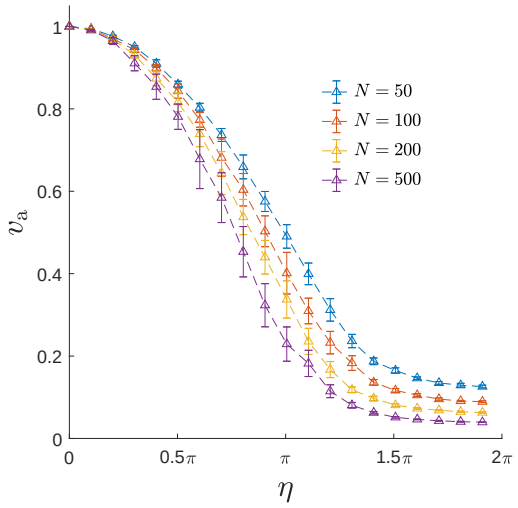

Figure 2.3: The normalized average velocity v_a is used as an order parameter for the Vicsek particle system. Studying the relation between it and the noise level, η, a clear phase transition from highly ordered to disordered is observed. The four curves show v_a for 50, 100, 200 and 500 particles respectively, all at the same particle density (2 particles/unit area). Despite having the same density, the different systems reach different levels of order in the unordered phase. These results are consistent with the ones obtained by Vicsek et al. when the model was first proposed (Vicsek et al., 1995). The error bars show one standard deviation for the block averages of v_a, taken from 20 blocks of 500 samples each.

2.2 Vicsek Model with Finite-Sized Particles

In the original Vicsek model, each particle is treated as a point particle. In systems where the interaction distance between particles is many orders of magnitude larger than their physical size, this approximation will affect the result very little as mostly far-away interactions matter, e.g. the electromagnetic interaction between the nucleus and the electrons. However, for other systems where these length scales are more similar, such as for bacteria or people moving through a crowd, effects of close-range interaction are not negligible. Very common forms of close-range interaction in many systems are friction and force arising from contact or collisions with other particles.

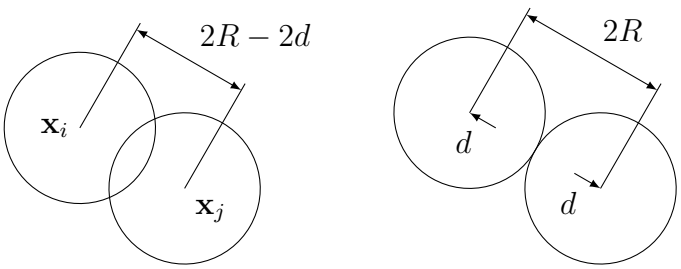

Figure 2.4: If two particles violate the volume exclusion condition and overlap, they will be equally displaced half the overlap length, along the center-to-center axis. The new particle positions, after displacement, are given by Equation (2.6).

Therefore a modified version of the Vicsek model will now be presented, with finite particle size. The modified model adds short-range interactions as a result of the finite extension in space of the particles, adding a volume exclusion condition. All particles are treated as hard spheres with radius $R < r$; for the model to work, it requires that the long-range interaction distance r is larger than the radius of the particles. The long-range interaction in Equation (2.2) is unaffected by this expansion. But if two particles, after being updated according to Equation (2.1), are close enough that they overlap, they will symmetrically be displaced half of the overlap length along the center-to-center axis. This is illustrated in Figure 2.4.

In further detail, this means that if $|\mathbf{x}_i - \mathbf{x}_j| < 2R$, $i \neq j$, particles i and j have collided. Both particles will then be displaced by d in opposite direction, where $|\mathbf{x}_i - \mathbf{x}_j| = 2R - 2d$. Explicitly this yields

$$2R - |\mathbf{x}_i - \mathbf{x}_j| = 2d \Rightarrow \frac{d}{|\mathbf{x}_i - \mathbf{x}_j|} = \frac{1}{2}\left(\frac{2R}{|\mathbf{x}_i - \mathbf{x}_j|} - 1\right) \tag{2.4}$$

and

$$\begin{aligned} \mathbf{x}_i &\to \mathbf{x}_i + \frac{d}{|\mathbf{x}_i - \mathbf{x}_j|}(\mathbf{x}_i - \mathbf{x}_j) \\ \mathbf{x}_j &\to \mathbf{x}_j + \frac{d}{|\mathbf{x}_i - \mathbf{x}_j|}(\mathbf{x}_j - \mathbf{x}_i). \end{aligned} \tag{2.5}$$

Combining (2.4) and (2.5), the positions of the particles will be updated to

$$\begin{aligned} \mathbf{x}_i &\to \frac{1}{2}\left(\frac{2R}{|\mathbf{x}_i - \mathbf{x}_j|} + 1\right)\mathbf{x}_i - \frac{1}{2}\left(\frac{2R}{|\mathbf{x}_i - \mathbf{x}_j|} - 1\right)\mathbf{x}_j \\ \mathbf{x}_j &\to -\frac{1}{2}\left(\frac{2R}{|\mathbf{x}_i - \mathbf{x}_j|} - 1\right)\mathbf{x}_i + \frac{1}{2}\left(\frac{2R}{|\mathbf{x}_i - \mathbf{x}_j|} + 1\right)\mathbf{x}_j. \end{aligned} \tag{2.6}$$

Ideally, the displacements from the volume exclusion (Figure 2.4) should be small. Otherwise there is a risk of displacing particles into other particles, resulting in impossible intermediate states and unstable and unreliable simulations, from which no conclusions can be drawn. As a result, this imposes the condition $d \ll R$. In the worst-case scenario, the overlap between two particles is $2d = 2v\Delta t$. With $\Delta t = 1$ in the Vicsek model, particle speeds that can reliably be simulated are restricted by $v \ll R$. Alternatively, the volume exclusion condition may be checked and enforced for interpolated times in numerical simulations, but since there is no explicit speed dependence in the model and Vicsek et al. (1995) found no qualitative change from varying v, this has the same effect as simulating the system for a lower speed.

2.2.1 Finite-size Vicsek Simulations

The additions to the Vicsek model proposed here are not expected to affect defining characteristics of such active systems. In fact, the desired outcome is the opposite, only systems where $r \approx R$ should be affected to a larger extent. To verify

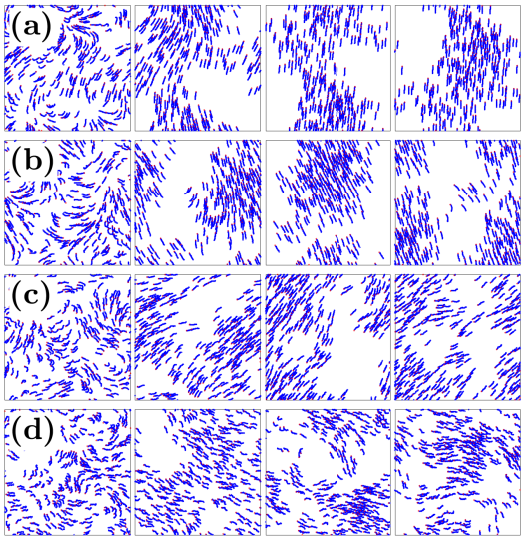

Figure 2.5: 400 particles simulated according to the finite-size model for different noise levels in a square space with side $L = 10$. The size of the particles is set to 0.1, so that $R \ll r = 1$. Similar to Figure 2.1, the panels show snapshots of the system at times 20, 100, 500 and 1,000. Above, simulations for noise levels (a) $\eta = 0.03\pi$, (b) $\eta = 15\pi$, (c) $\eta = 0.3\pi$ and (d) $\eta = 0.6\pi$ are shown. Comparing the results above to those of Figure 2.1 we see that the system dynamics (at high particle concentration) are not noticeably affected by the finite size of the particles. Particles appear less tightly packed than in the original model for high densities, which is expected from the finite-size addition.

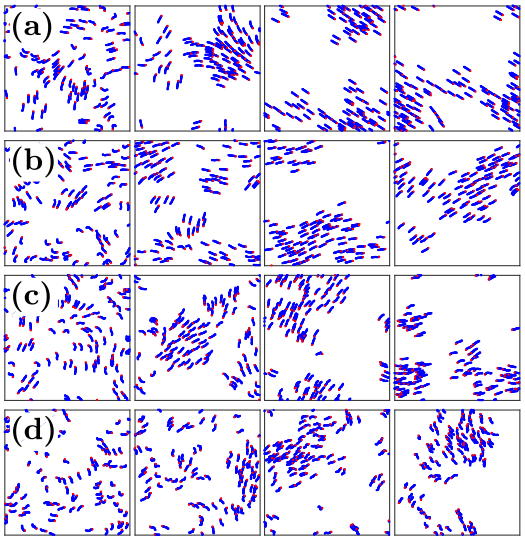

Figure 2.6: 100 particles simulated according to the finite-size model for different noise levels in a square space with side $L = 10$. The particle size $R = 0.1$, so that $R \ll r = 1$. The panels show snapshots of the systems at time 20, 100, 500 and 1 000. The noise levels in the simulations are (a) $\eta = 0.03\pi$, (b) $\eta = 0.15\pi$, (c) $\eta = 0.3\pi$ and (d) $\eta = 0.6\pi$ respectively. At low particle concentrations the result also seems unaffected by the finite size of the particles compared with Figure 2.2.

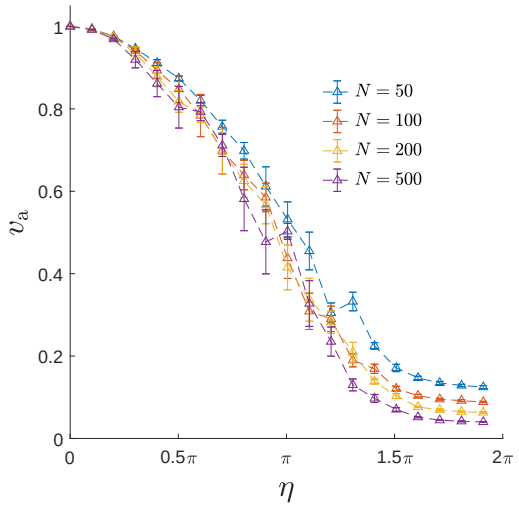

Figure 2.7: The normalized average velocity v_a is used as an order parameter for the Vicsek model with finite-sized particles. Comparing the result to the phase diagram in Figure 2.3, deviations from the phase diagram have clearly appeared and there seems to be a greater variance in the order parameter for the mid regions. For the most part, it seems the finite size of the particles has increased the order parameter in this region. Likely, this is an effect of particles being forced to be more spread out, mediating the interactions further in the system to a larger extent than in the original model. Despite this, the overall behaviour is preserved. The error bars show one standard deviation for the block averages of v_a taken from 20 blocks of 500 samples each.

that the behaviour has not been drastically altered, simulations where $R \ll r$ for systems similar to those in Figures 2.1 and 2.2 have been done, visualised in Figures 2.5 and 2.6. Qualitatively, no observable characteristics of the systems have changed. In the case of higher densities (Figure 2.5), the particles appear less tightly packed than in the original model (Figure 2.1). This is an expected result of the finite-size addition, but its effect on the system-wide qualitative behaviour is close to negligible.

Although, a side-effect of particles being more spaced out is an increased distance over which the aligning interactions are mediated over. This is more noticeable when comparing the order parameter of the two models (Figures 2.3 and 2.7). The overall look is the same, but the addition of finitely-sized particles appear to have increased the order parameter for the system in the mid-noise regions. The effect is only marginal however.

With these results, we draw the conclusion that the model has not been altered significantly, but with this addition can be examined in a complex environment, constituting active and passive particles.

Chapter 3

Active Particles in a Complex Environment

In this chapter, the expanded Vicsek model in Section 2.2 is examined in more complex environments and results from such simulations are presented and discussed. In light of these results, the self-organizing laning behaviour is compared to channel formation, leading to the development of a novel model for active particles. This model is presented in the next chapter.

3.1 Defining the Complex Environments

Whether collective behaviour of active particles or that of macroscopic agents is considered, the environment in which it takes place is an important aspect. Typically for active colloids, their interaction range is roughly in the order of magnitude of their size, which is why they cannot be described by point particles when studying their interactions with each other and the environment.

In Section 2.2 we modified the existing Vicsek model accordingly in order to apply it in a complex environment, rather than studying the inherent complexity of the system it describes. Two types of complex environments are considered here: a mixed system with a passive background and systems with two distinct "species" of active particles. The intrinsic scientific interest in the former is easy to motivate, as this type of system naturally occurs and it has been the subject of study in previous works, experimentally (Wu and Libchaber, 2000; Koumakis et al., 2013; Kümmel et al., 2015; Pinçe et al., 2016; Argun et al., 2016) and theoretically (Grégoire et al., 2001; Schwarz-Linek et al., 2012; Stenhammar et al., 2015).

The latter case, with two species of particles, has not been given the same attention to date. While no examples of naturally occurring colloidal systems described by this phenomenon are known, engineering similar behaviour for robotics is straightforward, if such systems exhibit desired behaviour.

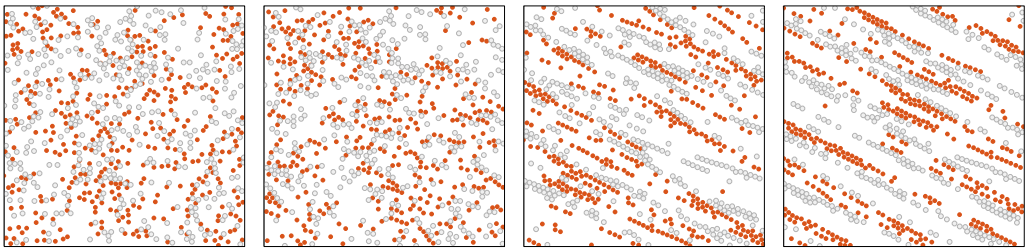

Figure 3.1: Snapshots at different times from a simulation of the modified Vicsek model in an environment of passive particles, showing the emergence of self-organizing lanes. The frames (left to right) correspond to times 20, 100, 500 and 1 000 in the same simulation. Orange circles denote the active Vicsek-particles. Grey ones denote passive, zero-speed particles that only interact via the close-range volume exclusion interaction of the modified Vicsek model, described in section 2.2. With a low level of noise ($\eta = 0.03\pi$), a lane-like structure emerges over time. The direction of the lanes is chosen spontaneously and differs between simulations. The particles (400 active and 400 passive) have a radius of $R = 0.1$ where the interaction range $r = 1$ is used as the characteristic length scale, and the square arena has a side of length $L = 10$.

3.2 Vicsek-like Particles in a Passive Environment

To model the passive environment, without interfering with the modified Vicsek-model used, together with the N active particles we place M passive ones. These are treated as zero-speed particles of the same size as the active ones. This means, that the aligning interactions of the Vicsek-model does not affect the passive particles and in turn, they do not affect the active ones. The volume exclusion condition (see Figure 2.4) still applies between passive-passive and active-passive particles though. Consequently, the presence of passive particles has no real impact on the order parameter examined in Chapter 2, which has been verified by simulations.

Running simulations for a crowded system at low noise levels, self-organizing laning behaviour emerges (Figure 3.1). This is reminiscent of results reported by Glanz and Löwen (2012), where passive particles driven in opposite direction by an external field form lanes. The direction of the lanes depends on the spontaneously chosen direction of motion of the active particles.

Moving into the high-noise regime these lanes vanish and no self-organization takes place. This is visualized in Figure 3.2.

3.3 Two "species" of Vicsek-particles

Exactly what a systems of distinct "species" of active particles means is not inherently clear. It could consist of particles interacting through vastly different mechanisms, mathematically modelled as well as physically. It could also refer to groups of particles interacting only within the group, effectively perceiving other

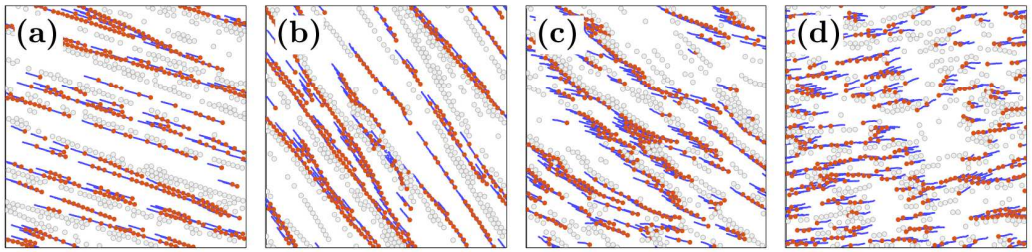

Figure 3.2: Snapshots from simulations of the modified Vicsek model in an environment of passive particles. Snapshots from simulations with noise levels (a) $\eta = 0.03\pi$, (b) $\eta = 0.15\pi$, (c) $\eta = 0.3\pi$ and (d) $\eta = 0.6\pi$ are shown above. As the noise increases the lanes break down and vanish. Orange circles denote active particles and particle trails are shown in blue. Grey circles denote passive particles.

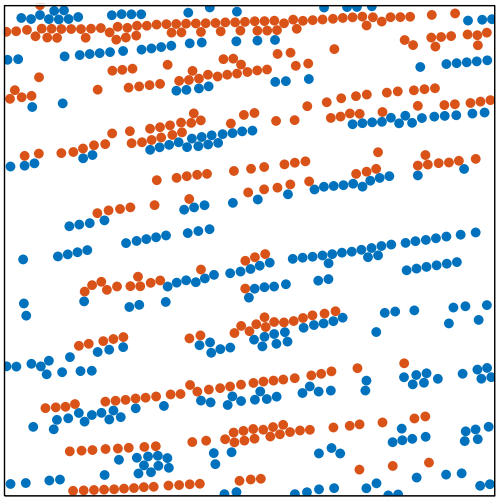

Figure 3.3: Snapshot from simulation of two "species" of active particles (denoted with different colours), which only interact with their own species, apart from volume exclusion. For low levels of noise, self-organizing laning occurs similar to that of Figure 3.1.

groups as passive. To really raise the complexity, we could imagine a system in which particles are allowed to transition to other species. In this thesis, the latter multi-species systems, without species-transitions, are considered.

Similarly to the result in a crowded environment, in the previous section, the two species will self-organize into forming lanes. Figure 3.3 shows this. Similar to the systems treated in Section 3.2, this only occurs in the low noise-regime and laning vanishes in the high noise-regime.

3.4 Self-organizing Behaviour

As the two previous sections showed, several examples of complex environments give rise to self-organizing laning, in active and passive systems alike, taking the results of Glanz and Löwen (2012) into account. This way, active particles could be used to improve the structuring of passive systems which do not reliably

respond to the effect of external fields. However, since it is not a phenomenon exclusive to active systems, its intrinsic scientific interest is somewhat diminished, in regards to theoretical models and descriptions of active matter.

A more interesting topic for studies of active matter would instead be the channelling behaviour displayed by e.g. biological systems. Looking at for example blood vessels, a type of biological channel, their physical appearance suggests there are more dynamic interactions at work than in these straight lanes. From the results presented here (Figures 3.1, 3.2 and 3.3), it appears that this is not accomplished without further interaction between active and passive particles and requires active particles being more "aware" of their environment. The Vicsek model does however not capture such mechanisms properly and the—probably—extensive modifications needed push the model too far from its original formulation to be desirable, likely with poor results. Moving too far from the simplicity of the Vicsek model goes against one of the main principles for modelling complex systems. A far better approach would be to formulate a new Vicsek-like model, that better incorporates such mechanisms in a concise way.

Chapter 4

A Novel Model of Active Particles

In this chapter a novel model of active particles is presented and explored. Somewhat inspired by the hydrodynamic interactions between active particles like microswimmers and bacteria suspended in fluid, torque-like aligning interactions are used. This particular model has not been used before in the literature and it exhibits a rich emergent behaviour, despite its simplicity. It is studied in purely active systems as well as mixed systems, constituted of both active and passive particles.

A scientific paper written on this particular model in connection with this thesis is available at `http://arxiv.org/abs/1706.01326` (Nilsson and Volpe, 2017).

4.1 Model Motivation

Many studies on active systems concern motile bacteria or microswimmers suspended in fluid, e.g. works by Wu and Libchaber (2000); Grégoire et al. (2001); Theurkauff et al. (2012). Hence, it is not unlikely that taking hydrodynamics into account would be fruitful in reproducing some of the effects observed. However, this approach goes against many of the principles of modelling collective behaviour mentioned in Chapter 1. Instead, inspiration has been drawn from hydrodynamics when constructing the aligning interactions constituting the model, to capture the essential elements of the mechanisms behind the complex behaviours observed in a simple way. The inter-particle interactions here have taken a torque-like form, dependent on the positions of neighbouring particles. Further details on these interactions are given in the next section.

The original Vicsek model uses velocity dependence for the local aligning interactions, but there are advantages to using position-dependent interactions, however. This is something also explored by Barberis and Peruani (2016). One of the advantages is the cheaper computational cost for measuring relative distance compared to computing relative or absolute velocity, when moving from simulations to real-world implementations, such as robotics. Additionally, de-

pending on the interaction-strength drop-off for larger distance, it is also more easily translated to natural sensory input, such as light intensity (Mijalkov et al., 2016) or concentrations of chemicals.

4.2 Mathematical Description of the Model

We consider N active particles moving continuously in 2 dimensions. The arena in which they are located is square-shaped and periodic boundary conditions are used. Similar to the case of the finite-sized Vicsek model in Section 2.2, we consider systems where the interaction range is roughly the order of magnitude of the particle size. Again, we consider them to be hard spheres; consequently the volume exclusion condition applies (see Section 2.2 and Figure 2.4 for details).

The particles reorient their direction of motion based on torque-like aligning interactions, which from now on will be referred to as "torque". The strength of the torque decreases with distance, so the importance of local interactions vastly outweighs that of those emanating from the global state of the system. The form of the applied torque is inspired by that of a hydrodynamic interaction. It is important to note, however, that no attempt to model a hydrodynamic interaction is made.

Let $\mathbf{x}_n(t)$ denote the position of particle $n = 1, \ldots, N$, at time t. Like the models presented by Vicsek et al. (1995); Barberis and Peruani (2016); Cambui et al. (2017) the particles are assumed to move with constant speed v, in the direction $\theta_n(t)$. Between times t and $t+1$, each particle n is updated according to

$$\begin{aligned} \theta_n(t+1) &= \theta_n(t) + T_n + \xi \\ \mathbf{x}_n(t+1) &= \mathbf{x}_n(t) + \mathbf{v}_n(t+1) \\ &= \mathbf{x}_n(t) + v\left(\cos\theta_n(t+1),\ \sin\theta_n(t+1)\right)^T . \end{aligned} \tag{4.1}$$

Here, ξ is a white-noise term, uniformly distributed on the interval $[-\eta/2, \eta/2]$ and T_n is the torque exerted on the particle. The torque T_n is given by

$$T_n = T_0 \sum_{i \neq n} \frac{\hat{\mathbf{v}}_n \cdot \hat{\mathbf{r}}_{ni}}{r_{ni}^2} \left(\hat{\mathbf{v}}_n \times \hat{\mathbf{r}}_{ni}\right)_z , \tag{4.2}$$

where $\mathbf{r}_{ni}$ is the relative position vector from particle n to particle i and $r_{ni} \equiv |\mathbf{r}_{ni}|$. A vector with a "hat" $\hat{\cdot}$ denotes a vector of unit length and $(\cdot)_z$ the z-component of a vector. T_0 is a parameter related to the strength of the aligning interaction, with $T_0 = 0$ corresponding to no aligning interactions, resulting in active Brownian motion. Active Brownian motion is also known as run-and-tumble dynamics, where the particles move in a straight line, followed by sudden, random reorientation after which they move again, and so on.

A visualization of this interaction can be found in Figure 4.1a. Figure 4.1b-i shows particle behaviour in a few simple cases, in the absence of orientational noise ($\eta = 0$). In general, we note that particles will tend to turn towards particles

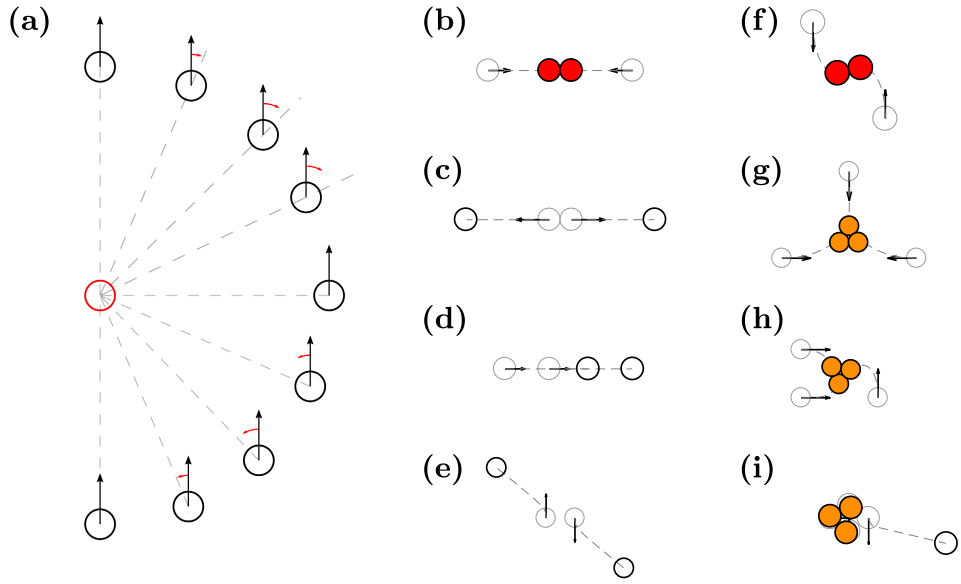

Figure 4.1: A visual representation of the interactions described in Eqs. (4.1) and (4.2). (a) The torque (red arc) exerted on a moving particle (black) by another particles (red) for different relative positions. Black arrows denote direction of motion. (b)-(i) Show particle behaviour for simple configurations in the absence of noise ($\eta = 0$). Coloured particles are part of a cluster; colour denotes cluster size. (b) Two particles starting facing each other will move in a straight line and form a 2-cluster. (c) Particles facing away will continue moving radially away from each other. (d) Particles oriented in the same direction continue moving in that direction in a straight line. (e) Particles with opposite orientation turn until they align and move apart, in a straight line. (f) Two particles turn towards each other until contact and form a 2-cluster. (g) Three particles, initially oriented towards a single point, move to form a 3-cluster. (h) Similar to (g) but with different initial velocities. (i) In a 4-cluster, one particle initially oriented 90° away from the centre leaves the cluster, while the remaining particles form a 3-cluster.

in front of them and away from those behind (4.1a). Additionally, we see that two particles oriented towards each other move to form a cluster of 2 particles (4.1b). If the are oriented away from each other or in the same direction (while in a line) they do not form a cluster (4.1c-d), instead they move apart radially or continue moving in a straight line, respectively. If the two particles are oriented in opposite directions, they will either form a 2-cluster or turn until they move apart in a straight line (4.1e-f). Figure 4.1g-h shows two initial conditions where three particles form a 3-cluster. Finally, a 4-cluster with one particle oriented at 90° away from the centre will lose that particle, but remain as a 3-cluster.

4.2.1 Cluster Detection

As noted from Figure 4.1b-i, this model describes the formation of clusters of particles. Clustering of active particles and the formation of crystal-like structures, as a phenomenon, has been observed experimentally by e.g. Theurkauff et al. (2012)and Palacci et al. (2013).

To properly analyse the formation, lifetime and, in particular, the existence of said clusters in simulations, clusters were identified using a "connected subgraph" approach. In further detail, this means that a snapshot of the system is taken at time t and a graph, with nodes n_i, $i = 1, ..., N$ placed at the particles' positions, is created. Node n_i and n_j are connected via an edge if and only if particle i and particle j are within 1.1 diameters (center-to-center).

This is compared to the result at a delayed time $t + \Delta t$. All connected subgraphs with at least one edge (at least two particles) are classified as clusters, given that they survive until $t + \Delta t$. The purpose of the delay is to not falsely classify particles as part of a cluster due to randomly being close at time t.

The connected subgraphs were found using the graph adjacency matrix A, which is defined with elements

$$A_{ij} = \begin{cases} 1 & \text{if } n_i \text{ and } n_j \text{ within 1.1 diameters and } i \neq j, \\ 0 & \text{otherwise.} \end{cases} \tag{4.3}$$

In turn, a cluster matrix C is computed using A. The elements of C are given by

$$C_{ij} = h\left(\left(\sum_{k=1}^{\infty} A^k\right)_{ij}\right), \text{ where } \quad h(x) = \begin{cases} 1 & \text{if } x > 0, \\ 0 & \text{otherwise.} \end{cases} \tag{4.4}$$

This means that $C_{ij} = 1$ if n_i and n_j are connected, and 0 otherwise. Clusters are found as the unique rows (or columns) of C with non-zero elements. In numerical simulations, mainly two options for computing C exist: using a truncated approximation

$$\tilde{C}_{ij} = h\left(\left(\sum_{k=1}^{k_{\max}} A^k\right)_{ij}\right), \tag{4.5}$$

corresponding to allowing a maximum number of steps between nodes in the graph, or evaluating $\tilde{C}$ for increasing $k_{\max}$ and stopping when the graph stops becoming more connected, or is fully connected. The former was used in this project, with a $k_{\max}$ of 5.

4.2.2 Cluster stability

From Figure 4.1 we concluded that there are circumstances where particles following the aligning interactions in Equations (4.1) and (4.2) form clusters, in the absence of noise ($\eta = 0$). Naturally, the question arises whether clusters form in a noisy system ($\eta > 0$), and if they are intrinsically stable once formed.

A maximally noisy system ($\eta = 2\pi$) has the orientation of each particle completely randomised at each timestep, resulting in active Brownian motion. Clustering is not observed in simulations of active Brownian motion without any further interactions (Volpe et al., 2014; Bechinger et al., 2016). Thus, we do not expect clusters to appear in a maximally noisy system. Consequently, we expect to see a behavioural phase-transition at some intermediary noise level.

Disregarding the particle speed v for now, the parameters of the model are η, T_0 and R (the particle radius). The speed will be discussed in the next section. However, regarding the cluster stability they are all coupled. Looking at Equation 4.2, it is easy to realise that torque between two particles is strongest at contact, i.e. in a cluster. Considering only the interaction between those particles, the torque becomes

$$T_n = T_0 \frac{\hat{\mathbf{v}}_n \cdot \hat{\mathbf{r}}_{ni}}{4R^2} \hat{\mathbf{v}}_n \times \hat{\mathbf{r}}_{ni} = \frac{T_0}{4R^2} \sin\varphi \cos\varphi, \tag{4.6}$$

φ being the angle between the velocity and the relative position. The maximum value of $\sin\varphi\cos\varphi$ is easily found as $1/2$, yielding

$$T_n \leq \frac{T_0}{8R^2} = T_{\max}. \tag{4.7}$$

From Equation (4.7), a critical level of noise can be found where the noise is capable of cancelling the effect of any single particle,

$$\frac{\eta_c}{2} = T_{\max} \Rightarrow \eta_c = \frac{T_0}{4R^2}. \tag{4.8}$$

At this noise level, we expect clusters to potentially destabilize. Following this reasoning, the expected phase-transition is likely to take place in this region, since for $\eta > \eta_c$ the more likely clusters are to destabilize the larger the difference is.

4.3 Simulations of Purely Active Systems

The model described above has been explored using numerical simulations in Matlab. The main focus has been the expected phase-transition between clustering and non-clustering behaviour. As explained in Section 4.2.2, this couples most of the parameters of the model (see Equation (4.8)). Therefore, both T_0 nd R have been fixed: $T_0 = 1$, $R = 1$. The model is not expressed in any particular length or time scale, which should be evaluated on a implementation-to-implementation basis. Hence, all parameters are considered only numerically in these results and

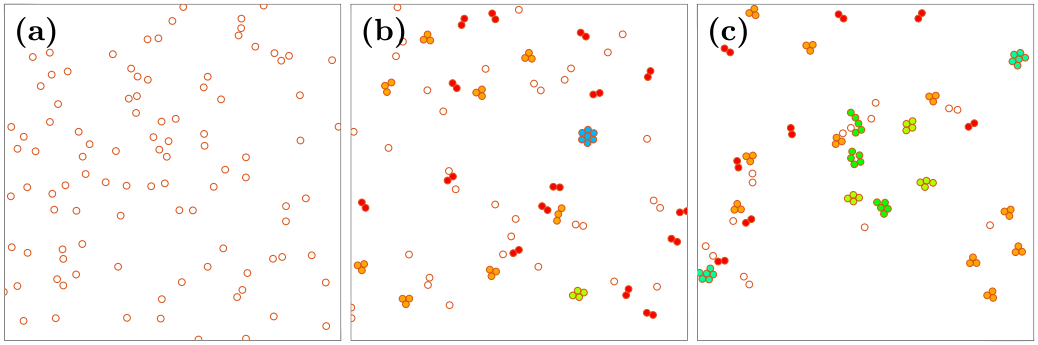

Figure 4.2: Snapshots from simulations of $N = 100$ active particles for different noise levels. The noise levels are $\eta = 2\pi$, $\eta = 0.2\pi$ and $\eta = 0.002\pi$ respectively. Particles in clusters are coloured depending on the size of the cluster: 2 (red), 3 (orange), 4 (light green), 5 (green), 6 (dark green) and 7 (blue). (a) In a maximally noisy system, we see that clusters do not form and instead the system exhibits a gas-like behaviour, or gaseous state. Due to randomness, particles will sometimes get close enough to form a 2-cluster. However, they do so rarely and the clusters are extremely short-lived and dissolve almost immediately. (b) As noise decreases, most particles form clusters. The smaller clusters of two or three particles are by far the most common. Larger clusters are also present, but with lower frequency. (c) At very low levels of noise, almost every particle is part of a cluster. The larger clusters have become more frequent and as a result, the smaller clusters have decreased in number slightly.

discussions. Although, the focus on colloids and microswimmers in its development and motivation suggests "typically short" length and time scales.

The only parameter left uncoupled by Equation 4.8 is the particle speed v. The speed itself is not present in the formulation of the aligning interactions (Equation (4)) and within reasonable boundries, it does not qualitatively affect the behaviour of the system in any interesting way, as reported by Vicsek et al. (1995). In our case, due to the time-discrete nature of the model, we speculate that a larger v would result in a smaller effective T_0, since particles would move further along any particular direction before their orientation is altered. For this reason, v has also been fixed.

Due to the volume exclusion constraint being enforced with particle displacements at every timestep, this requires that the displacement $d \ll R$ (see Figure 2.4). In the worst case scenario $d = v\Delta t = v$, in turn requiring that $v \ll R$. Therefore, $v = 0.05$ has been used in all simulations.

Using the parameter values above, for varying η, behaviour like that presented in Figure 4.2 is observed. For very noisy systems, like Figure 4.2a, motion is almost gaseous and clusters don't tend to form, as expected from the reasoning in Section 4.2.2. Due to randomness, particles will sometimes come close enough to form a cluster, but they very quickly move apart again and the cluster vanishes. Lowering the noise level a bit, smaller clusters start to form, typically 2- and 3-clusters. Decreasing the noise further, the larger clusters start appearing and less particles move around on their own. The lower the noise, the more frequent the larger clusters become and as a consequence, the frequency of the smaller clusters also decreases. This is visualized in Figure 4.3b.

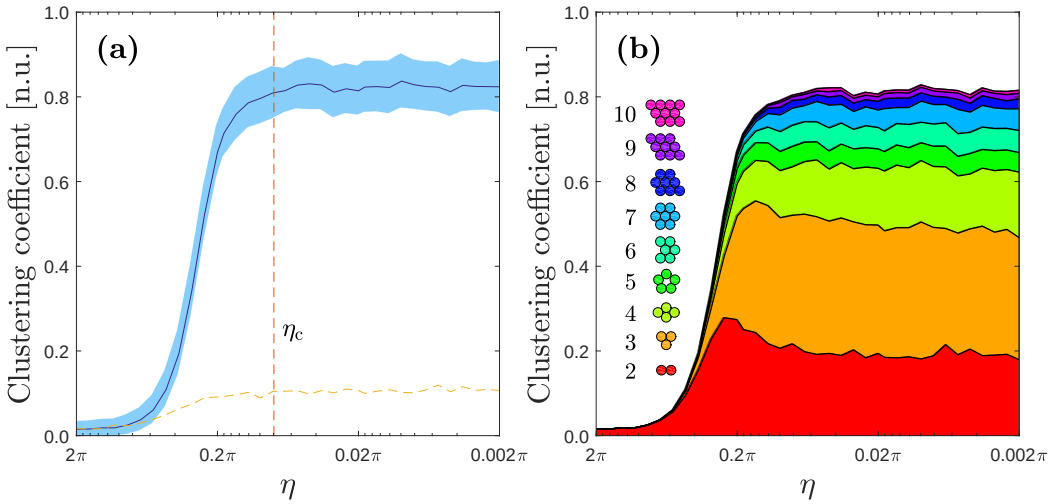

Figure 4.3: The clustering coefficient (defined as the fraction of particles that are part of clusters) clearly shows the transition between a clustering state and the more gaseous one in Figure 4.2a. (a) The mean clustering coefficient, taken from simulations of 10^5 timesteps, is shown for different values of η. The standard deviation is shown by the shaded area. This is compared to the baseline case, where $T_0 = 0$, i.e. no aligning interaction takes place (the yellow dashed line). The baseline case is significantly lower, indicating that clustering indeed is a result of the aligning interactions in Equations (4.1) and (4.2). The critical noise level η_c (Equation (4.8)) is also marked as the vertical dashed line. As expected, for $\eta > \eta_c$ a steep decline in the clustering coefficient is observed. (b) Cluster size distribution as a function of η. The colours correspond to the sizes of the clusters shown as insets. We see that the first clusters to form, and also the most frequent, are 2- and 3-clusters. Larger clusters begin to form later, and at lower levels of noise they increase in frequency, naturally lowering the frequency of smaller clusters.

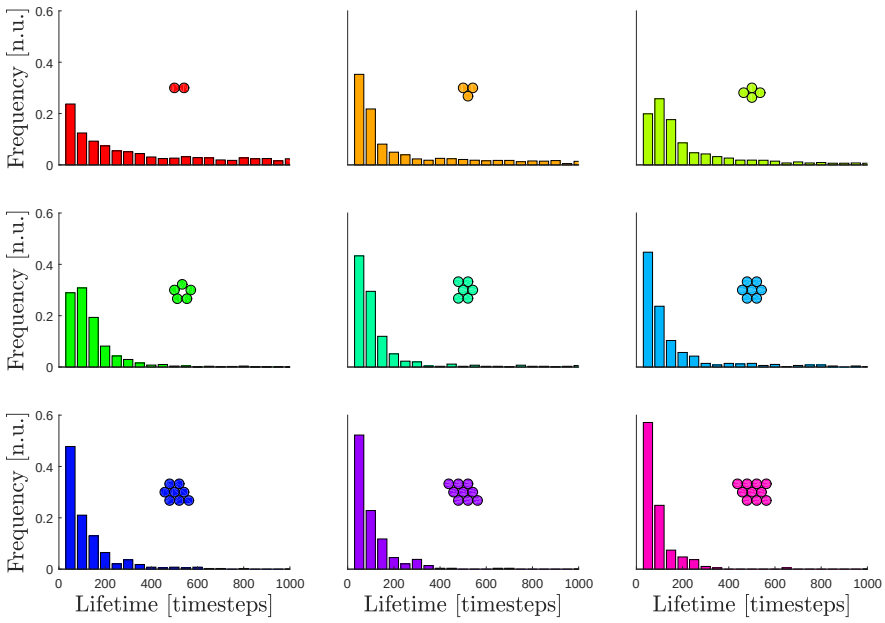

Figure 4.4: The lifetime of different clusters varies depending on their size. Lifetime distributions are shown for $\eta = 0.003\pi$. Clusters are shown as insets in the corresponding distribution.

Looking at the fraction of particles that are part of a cluster, we get a suitable measure for the degree of clustering in the system. This clustering coefficient is used as our order parameter to study the phase-transition in Figure 4.3. As shown in the figure, a clear transition occurs as η varies. Also noteworthy is the fact that for $\eta > \eta_c$ there is a steep decline. It appears that clusters rapidly become less and less stable, which agrees with the reasoning in Section 4.2.2.

Looking closer at the evolution and lifetime of different clusters, lifetime distributions can be found in Figure 4.4. The most common transitions between different cluster sizes are also visualized as a transition network in Figure 4.5.

4.4 Exploring the Model in a Crowded, Mixed Environment

So far, all systems explored have been purely active, consisting of only active particles. Many systems in reality, however, are constituted of active as well as passive particles. It has also been shown that a few active particles in an otherwise passive system, or vice versa, can alter or affect the behaviour of the system by Wu and Libchaber (2000) among others. Several other works have also explored this experimentally (Koumakis et al., 2013; Kümmel et al., 2015; Pinçe et al., 2016; Argun et al., 2016) and theoretically (Grégoire et al., 2001; Schwarz-Linek et al., 2012; Stenhammar et al., 2015).

In this section we look at the how the model has been explored in a crowded,

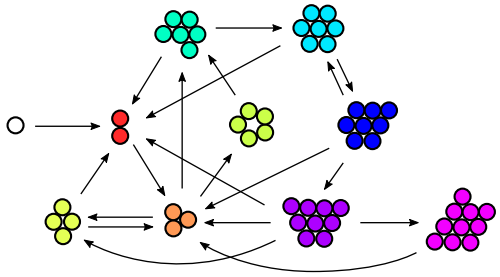

Figure 4.5: A cluster size transition network. The most common transitions are represented by arrows. The most stable clusters are those of size 2, 3, 6 and 7; in particular, they appear to be stable in the absence of external perturbations, i.e. collisions with other particles. Two-way transitions can often be observed between clusters of size 3-4 and 7-8, as shown by the double arrows between them.

complex environment of passive particles. For this reason, systems of N active particles together with M passive particles have been simulated. Passive particles only display diffusive motion, modelled by adding Gaussian white noise to their current position, but otherwise interact with other particles (active and passive) via volume exclusion. The variance of the Gaussian noise is set to $\sigma = 0.1v$, so that each timestep their displacement is much smaller than that of the active particles. The passive particles are assumed to be spherical and of the same size as active particles.

With model formulation from Section 4.2, the model does not incorporate any possibility for active particles to interact with the passive environment, disregarding the volume exclusion. The interplay between active and passive particles is not a phenomenon that can be completely neglected, though. We will therefore extend the model to account for active-passive interactions. Equation (4.1) remains unchanged, but T_n is instead given by

$$T_n = T_0 \sum_{i \neq n} \frac{\hat{\mathbf{v}}_n \cdot \hat{\mathbf{r}}_{ni}}{r_{ni}^2} \left(\hat{\mathbf{v}}_n \times \hat{\mathbf{r}}_{ni}\right)_z - T_0 \sum_{m} \frac{\hat{\mathbf{v}}_n \cdot \hat{\mathbf{r}}_{nm}}{r_{nm}^2} \left(\hat{\mathbf{v}}_n \times \hat{\mathbf{r}}_{nm}\right)_z , \tag{4.9}$$

where $m = 1, ..., M$ is the index of the passive particles and $\mathbf{r}_{nm}$ is the relative position between the active particle n and the passive particle m. The sign of the torque due to passive particles is negative so that active particles tend to avoid the passive ones. This "obstacle avoidance" behaviour is observed, for example, in the motion of people across a stationary crowd, shown by Helbing et al. (2005), and in the motion of microswimmers in the presence of obstacles (Takagi et al., 2014; Spagnolie et al., 2015). Additionally, obstacle avoidance is an important aspect of many robotic applications.

At low concentrations of passive particles ($M < N$) and at low packing fractions, the overall qualitative behaviour of the active particles is largely unaffected; active particles still form clusters as explained previously.

The effects of passive particles are more interesting at very high concentrations ($M \gg N$) and packing fractions, giving rise to phenomena such as channel forming. This is shown in Figure 4.6. The motion of the active particles is quantitat-

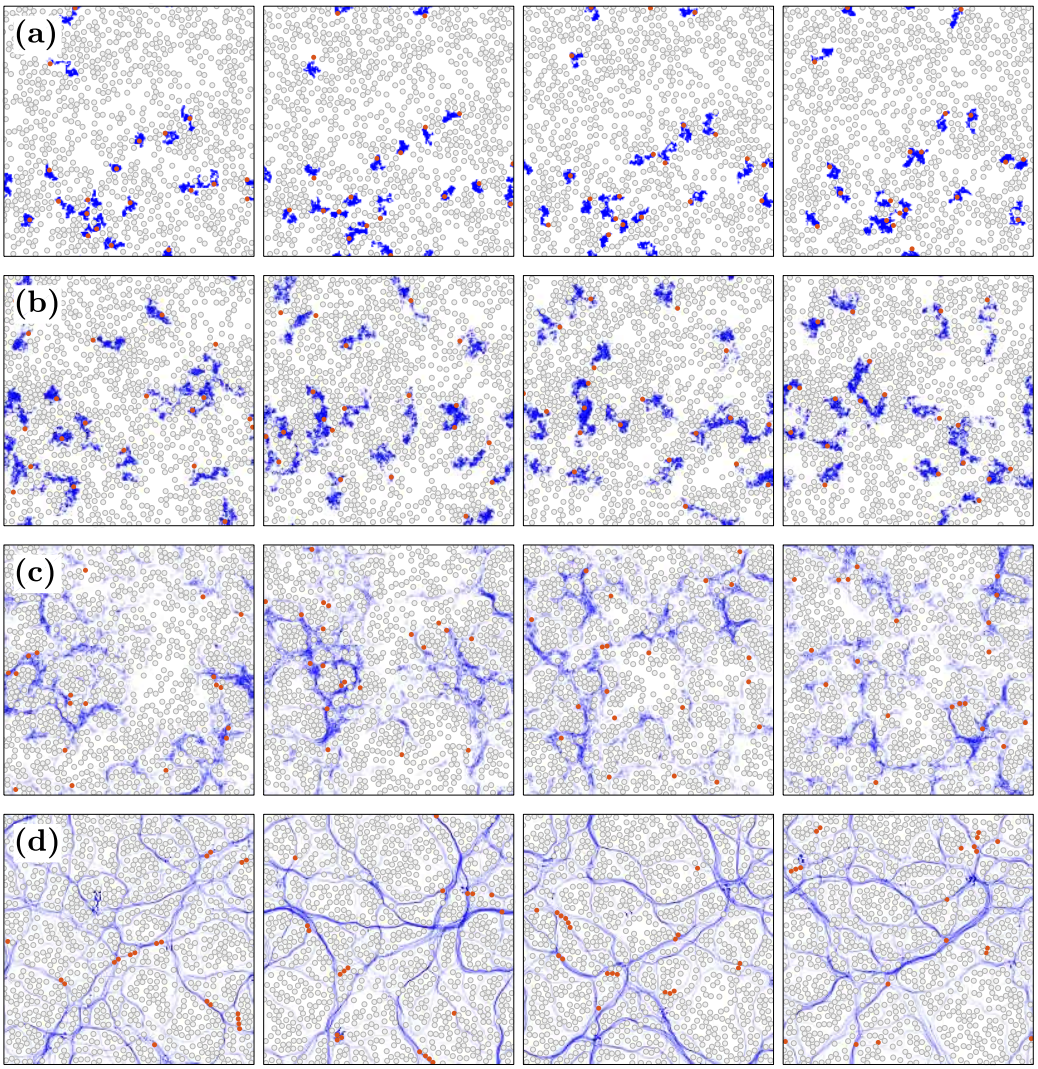

Figure 4.6: In crowded, mixed systems, channels form at lower levels of noise. Systems of 20 active particles (orange circles) and 900 passive (grey circles) have been simulated for for different values of η: (a) $\eta = 2\pi$, (b) $\eta = \pi$, (c) $\eta = 0.5\pi$ and (d) $\eta = 0.03\pi$. Particle trails for the preceding 25 000 timesteps are shown in blue. The frames correspond to times 25 000, 50 000, 75 000 and 100 000 (left to right). In (d), we observe the formation of metastable channels.

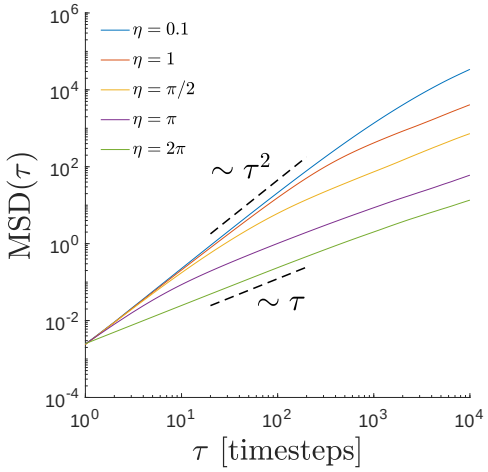

Figure 4.7: The mean square displacement of the active particles in systems like in Figure 4.6. Diffusive motion results in a mean square displacement evolution following a linear trend, while the trend for ballistic motion closer resembles τ^2 in the short term (Volpe et al., 2014; Bechinger et al., 2016; Howse et al., 2007).

ively examined using their mean square displacement,

$$\mathrm{MSD}(\tau) = \left\langle |\mathbf{x}_n(t+\tau) - \mathbf{x}_n(t)|^2 \right\rangle_n , \tag{4.10}$$

in Figure 4.7. In previous works, authors Volpe et al. (2014); Bechinger et al. (2016); Howse et al. (2007) have looked at motion transition utilizing that for diffusive motion $\mathrm{MSD}(\tau) \propto \tau$, while ballistic motion results in $\mathrm{MSD}(\tau) \propto \tau^2$.

Again, in a maximally noisy system ($\eta = 2\pi$, Figure 4.6a) the motion of the active particles is essentially diffusive, as they are hindered by the presence of passive particles. This is indicated by the mean square displacement of the particles, shown in Figure 4.7 (the green line). It has a slope close to 1 at all times, which is indicative of diffusive motion. The active particles compress the passive ones creating some voids within the background of passive particles, within which they are effectively confined. As a consequence, the active particles have few chances of encountering each other and forming clusters. This behaviour is similar to that of microswimmers in experiments conducted by Kümmel et al. (2015), where their presence in a passive bath, even at very low numbers, could help the crystallisation of the system.

Decreasing the noise to $\eta = \pi$ (Figure 4.6b), the active particles are able to move more, but remain confined within depletion regions created in the background of passive passive particles. Even though they can make some straight runs, they quickly become blocked by the passive particles and their movement quickly becomes diffusive. This is reflected by the MSD shown by the purple line in Figure 4.7, which after a brief superdiffusive stage for short times quickly becomes diffusive. Also in this case, the passive particles present in the background prevent encounters between active particles and the formation of clusters.

A similar behaviour takes place even for lower noise levels ($\eta = 0.5\pi$, Figure 4.6c). However, we can now observe the formation of some proto-channels. These

proto-channels permits active particles to occasionally meet and form 2-particle clusters.

Decreasing the noise level even further to $\eta = 0.03\pi$ (Figure 4.6) leads to the formation of fully-fledged channels, whose presence are clearly shown by the blue particle trails. These are areas free of passive particles where the active particles can propagate unhindered. Comparing the different panels of Figure 4.6d, which correspond to non-overlapping time frames, one can see that the channels are quite stable over time. The reason for this is that, once a channel is opened by some active particles, additional active particles use it leading to its dynamical stabilisation. This transition towards the formation of channels is driven by the increase of characteristic length of the directed runs the active particles in the background of passive particles. As can be seen from the blue line in Figure 4.7, the MSD is now ballistic over a longer time range. Once channels are open the particles can encounter each other and form some small (2- or 3-particle) clusters.

Chapter 5

Concluding Remarks

This thesis has studied collective behaviour in complex environments. At first the well-known Vicsek model was considered and expanded to allow for its use in systems where interaction range and particle size are roughly of the same order of magnitude. Exploring the modified Vicsek model in complex environments, self-organizing lane patterns were discovered. Not an inherent phenomenon of only active systems, attention was instead directed towards dynamical channels rather than straight lanes. To accommodate for the interactions between active and passive particles, the Vicsek model was abandoned in favor of a new Vicsek-like model developed during this thesis. This particular model manages to capture clustering behaviour and, with a slight modification, the forming of channels in a crowded, complex environment.

How well the model in Chapter 4 describes any real systems of active particles or collective behaviour remains to be seen. Nevertheless it has, in its current formulation, clearly captured some important aspect, or aspects, of how or why clustering and channelling occurs. If future research chooses to build upon this or take on a new approach only time can tell.

Regarding engineered systems, such as in robotics or specialised microswimmers, whether the result is identical to anything existing becomes less relevant and instead we look for potential applications. For example, real-time modulation of model parameters, such as noise or interaction strength, in a robotic system could utilize the behavioural phase-transition to switch between aggregation and exploration. This is achievable in what we refer to as purely active systems as well as mixed systems (Figures 4.2 and 4.6 respectively). Similarly, external fields could be used to modulate the stability of clusters of microswimmers locally as a method of manufacturing crystal-like structures. Alternatively, this kind of microswimmers could be used to design blood-vessel networks for bio-tissue printing, or similar.

In Chapter 3 we were quick to abandon the Vicsek model for these types of complex environments, but I don't believe that area of research is exhausted even if, within the scope of this thesis, a different approach was chosen. Furthermore, the newly developed model has, as it stands, not been explored fully. In the future, further study of this model in larger and more complex systems would be an

interesting research project. The concept of particle species or types, in particular, is something not currently found in the literature, even for successful models like the Vicsek model. Looking at active biological systems like the immune system, where its different agents are separated to perform specific tasks, it's an approach that I believe could be fruitfully explored. It is also possible to expand the model to 3 dimensions.

To conclude, the model developed in this thesis would be interesting to study further and the study of active particles in complex environments is an important area of research for many applications of active particles, e.g. nanorobotics and in medicine. Collective behaviour on the macroscopic scale is a growing field as well, with many potential applications, and research on collective behaviour may prove crucial for tackling many of today's or tomorrow's problems.

Bibliography

Argun, A., Moradi, A.-R., Pinçe, E., Bagci, G. B., Imparato, A., and Volpe, G. (2016). Non-boltzmann stationary distributions and nonequilibrium relations in active baths. *Phys. Rev. E*, 94(6):062150.

Barberis, L. and Peruani, F. (2016). Large-scale patterns in a minimal cognitive flocking model: Incidental leaders, nematic patterns, and aggregates. *Physical Review Letters*, 117(24):248001.

Bechinger, C., Di Leonardo, R., Löwen, H., Reichhardt, C., Volpe, G., and Volpe, G. (2016). Active particles in complex and crowded environments. *Reviews of Modern Physics*, 88(4):045006.

Brambilla, M., Ferrante, E., Birattari, M., and Dorigo, M. (2013). Swarm robotics: a review from the swarm engineering perspective. *Swarm Intelligence*, 7(1):1–41.

Cambui, D. S., Godoy, M., and de Arruda, A. (2017). Finite-size effects in simulations of self-propelled particles system. *Physica A: Statistical Mechanics and its Applications*, 467:129–136.

Czirók, A., Ben-Jacob, E., Cohen, I., and Vicsek, T. (1996). Formation of complex bacterial colonies via self-generated vortices. *Phys. Rev. E*, 54(2):1791.

Gautrais, J., Ginelli, F., Fournier, R., Blanco, S., Soria, M., Chaté, H., and Theraulaz, G. (2012). Deciphering interactions in moving animal groups. *PLoS Comput. Biol.*, 8(9):e1002678.

Ginot, F., Theurkauff, I., Levis, D., Ybert, C., Bocquet, L., Berthier, L., and Cottin-Bizonne, C. (2015). Nonequilibrium equation of state in suspensions of active colloids. *Phys. Rev. X*, 5(1):011004.

Glanz, T. and Löwen, H. (2012). The nature of the laning transition in two dimensions. *Journal of Physics: Condensed Matter*, 24(46):464114.

Grégoire, G., Chaté, H., and Tu, Y. (2001). Active and passive particles: Modeling beads in a bacterial bath. *Phys. Rev. E*, 64(1):011902.

Helbing, D., Buzna, L., Johansson, A., and Werner, T. (2005). Self-organized pedestrian crowd dynamics: Experiments, simulations, and design solutions. *Transportation Sci.*, 39(1):1–24.

Howse, J., Jones, R., Ryan, A., Gough, T., Vafabakhsh, R., and Golestanian, R. (2007). Self-motile colloidal particles: from directed propulsion to random walk. *Phys. Rev. Lett.*, 99(4):048102.

Koumakis, N., Lepore, A., Maggi, C., and Di Leonardo, R. (2013). Targeted delivery of colloids by swimming bacteria. *Nature Commun.*, 4:2588.

Kümmel, F., Shabestari, P., Lozano, C., Volpe, G., and Bechinger, C. (2015). Formation, compression and surface melting of colloidal clusters by active particles. *Soft Matter*, 11(31):6187–6191.

Mijalkov, M., McDaniel, A., Wehr, J., and Volpe, G. (2016). Engineering sensorial delay to control phototaxis and emergent collective behaviors. *Phys. Rev. X*, 6:011008.

Nilsson, S. and Volpe, G. (2017). Metastable clusters and channels formed by active particles with aligning interactions. arXiv:1706.01326.

Palacci, J., Sacanna, S., Steinberg, A., Pine, D., and Chaikin, P. (2013). Living crystals of light-activated colloidal surfers. *Science*, 339(6122):936–940.

Peruani, F., Deutsch, A., and Bär, M. (2006). Nonequilibrium clustering of self-propelled rods. *Physical Review E*, 74(3):030904.

Pinçe, E., Velu, S. K. P., Callegari, A., Elahi, P., Gigan, S., Volpe, G., and Volpe, G. (2016). Disorder-mediated crowd control in an active matter system. *Nature Commun.*, 7:10907.

Reynolds, C. W. (1987). Flocks, herds and schools: A distributed behavioral model. *ACM SIGGRAPH computer graphics*, 21(4):25–34.

Schwarz-Linek, J., Valeriani, C., Cacciuto, A., Cates, M., Marenduzzo, D., Morozov, A., and Poon, W. (2012). Phase separation and rotor self-assembly in active particle suspensions. *Proceedings of the National Academy of Sciences*, 109(11):4052–4057.

Spagnolie, S. E., Moreno-Flores, G. R., Bartolo, D., and Lauga, E. (2015). Geometric capture and escape of a microswimmer colliding with an obstacle. *Soft Matter*, 11(17):3396–3411.

Stenhammar, J., Wittkowski, R., Marenduzzo, D., and Cates, M. (2015). Activity-induced phase separation and self-assembly in mixtures of active and passive particles. *Phys. Rev. Lett.*, 114(1):018301.

Takagi, D., Palacci, J., Braunschweig, A. B., Shelley, M. J., and Zhang, J. (2014). Hydrodynamic capture of microswimmers into sphere-bound orbits. *Soft Matter*, 10(11):1784–1789.

Theurkauff, I., Cottin-Bizonne, C., Palacci, J., Ybert, C., and Bocquet, L. (2012). Dynamic clustering in active colloidal suspensions with chemical signaling. *Phys. Rev. Lett.*, 108(26):268303.

Vicsek, T., Czirók, A., Ben-Jacob, E., Cohen, I., and Shochet, O. (1995). Novel type of phase transition in a system of self-driven particles. *Physical review letters*, 75(6):1226.

Vicsek, T. and Zafeiris, A. (2012). Collective motion. *Phys. Rep.*, 517(3):71–140.

Volpe, G., Gigan, S., and Volpe, G. (2014). Simulation of the active brownian motion of a microswimmer. *American Journal of Physics*, 82(7):659–664.

Wahde, M. (2008). *Biologically inspired optimization methods: an introduction.* WIT press.

Wang, J. and Gao, W. (2012). Nano/microscale motors: biomedical opportunities and challenges. *ACS nano*, 6(7):5745–5751.

Wu, X. and Libchaber, A. (2000). Particle diffusion in a quasi-two-dimensional bacterial bath. *Phys. Rev. Lett.*, 84(13):3017.